Modelling Conductor Life Expectancy for HTLS Conductors

Haoji Liu, Konstantinos Kopsidas, Mohammed Al Aqil
Department of Electrical and Electronic Engineering
The University of Manchester
Manchester, UK
{haoji.liu, k.kospdias, m.alaqil}@manchester.ac.uk

2021 IEEE Power & Energy Society General Meeting (PESGM) | 978-1-6654-0507-2/21/$31.00 ©2021 IEEE | DOI: 10.1109/PESGM46819.2021.9637822

***Abstract*—Wind induced overhead conductor motions affect the conductors' life expectancy. Consequently, it is important to consider the differences in conductor structure among different conductor technologies. This paper introduces a model to calculate life expectancy for conventional aluminium-conductor steel-reinforced (ACSR) and a novel high-temperature low-sag (HTLS) aluminium conductor composite core (ACCC) based on the energy balance principle (EBP). Furthermore, various clamping locations of Stockbridge damping system are implemented to quantify the damping mechanism's efficiency and optimize its location. The EBP is implemented in two conductors of the same size but different technology (i.e., 495/35 ACSR and Rome ACCC). The study showed a 25% less bending stress of ACCC and thus approximately 5 times longer life from its equivalent (in diameter) ACSR, or alternatively increase ACCC tension by 6% RBS and allow higher overhead lines (OHLs) power transfer capacity. When the vibration dampers are installed inappropriately onto ACCC, by considering its response to be the same to its equivalent ACSR, ACCC's life expectancy is reduced by approximately 30%. To further understand the importance of HTLS conductor structure on its life expectancy, a semi-analytical EBP model is proposed based on experimental data on ACCC. The initial results show the great effect of conductor bending stiffness on ACCC life expectancy. Future experiments are needed to improve the EBP modelling and the HTLS conductor performance calculations.**

***Index Terms*—Aluminium Conductor Composite Core, Bending stress, Energy Balance Principle, Life expectancy, Overhead line conductor**

I. Introduction

In recent decades, electricity energy demand has been increasing rapidly all over the world [1], leading to the congestion of transmission overhead lines (OHLs). The novel high-temperature low-sag (HTLS) conductors, such as aluminium conductor composite core (ACCC), are gaining popularity because they can almost double the ampacity without causing more sag compared to the existing all aluminium alloy conductor (AAAC) or aluminium conductor steel-reinforced (ACSR) at same diameters [2]. OHLs and dampers are the key components to reliably deliver electricity [3]. However, conductor strands fatigue and failure occur due to aeolian vibration, which is a phenomenal motion induced by wind [4]. Although the vibration damper can dramatically reduce the vibration amplitude, the fretting fatigue failure usually occurs at or near the location of fittings and accessories in the vicinity of the clamp. It is important to understand the vibration and fatigue performance of HTLS conductor, for example, ACCC where its tensile strength on the aluminium and core are transferable due to the knee-point temperature effect. The design of OHL based on proper modelling of aeolian vibrations leads to improving the transmission line ampacity, and long-term service life when re-conductoring OHLs with HTLS conductors.

At present, many numerical models have been developed to calculate the OHL conductor aeolian vibration amplitude. The most common modelling method is the use of EBP. This principle interprets the wind-conductor interaction in a way that the imparted power from wind is equal to the power dissipated by conductor self-damping plus the power dissipated by vibration dampers [5]. EBP is used in [6]–[9] to calculate the aeolian vibration amplitudes for conventional conductors. To investigate the aeolian vibration of single conductor with multiple dampers, the studies in [10] and [11] use EBP to avoid solving a complex eigenvalue problem of damper modelling. Works have also been done to improve the performance of EBP by experimental data. The works in [12], [13] implement a series of experimental tests of the damper by test span and forced vibration method for the modelling of dampers and compare the experimental data to the results from EBP conductor vibration model.

To predict the damper power dissipation and conductor vibration, a nonlinear time history model and finite-element method are used to simulate the damper behaviour and optimize the existing EBP model [14]–[16]. The field data can also help the optimization of the conductor vibration modelling in terms of conductor self-damping performance [17]. Apart from the EBP method, the Finite Particle Method is also employed to calculate the response of aeolian vibration of conductor and damper's dynamic characteristics [18]. With the vibration amplitude obtained from the mentioned methods,

the conductor fatigue life can be estimated by fracture mechanics method combined with Miner linear damage theory [6], [19].

So far, the EBP is widely used by utilities for aeolian vibration calculations considering the conventional conductors with dampers. However, there are limited studies that model the performance of HTLS conductors. Additionally, there is still no comprehensive modelling for HTLS conductor life expectancy estimation and its performance in different conditions, for example varying tension or operating temperature (i.e., knee-point effect).

This paper examines the aeolian vibration and fatigue performances of HTLS conductors and proposes a novel model, based on ACCC experimental data, to improve the EBP modelling accuracy. The rest of the paper is structured as follows: Section II summarises the calculation methods of conductor aeolian vibration amplitude and the associated vibration fatigue. The methods are implemented for conventional ACSR and HTLS ACCC in Section III, with a few key assumptions enabling the latter one. Section IV proposes a semi-analytical framework aiming at enhancing the EBP modelling accuracy for HTLS conductors using experimental data. Conclusions and suggested future work are summarized in Section V.

II. Modelling of Conductor Vibration Bending Stress and Life Expectancy

This section demonstrates the modelling methodology of aeolian vibration using EBP, as shown in (1). Other factors like corrosion could affect life expectancy of the conductor but they have neglected in this modelling methodology as in most cases vibration fatigue is one of the most common factors that reduces conductor life-time, particularly for OHL systems installed away from coastal areas.

$$P_W = P_C + P_D \tag{1}$$

Where the element of P_W, P_C, and P_D are the induced wind power, conductor self-camping power and damper dissipated power, detailed in subsections II.A, II.B, and II.C, respectively. Equation (1) can be solved by iterative calculations assuming the maximum vibration amplitude is not greater than the conductor diameter. The estimated life expectancy is explained in subsection II.D using Miner's damage theory shown in (2) [20].

$$\mathrm{Dam} = \sum_i \mathrm{Dam}_i = \sum_i \frac{n(\Delta\sigma_i)}{N(\Delta\sigma_i)} \tag{2}$$

Where Dam is the total fatigue damage, $\Delta\sigma_i$ is the range of bending stress, $n(\Delta\sigma_i)$ is the number of cycles of alternating stress, and $N(\Delta\sigma_i)$ is the number of alternating stress cycles required for conductor breakage.

A. Induced Wind Power

The wind power transfer to the vibrating conductor P_W can be expressed by (3).

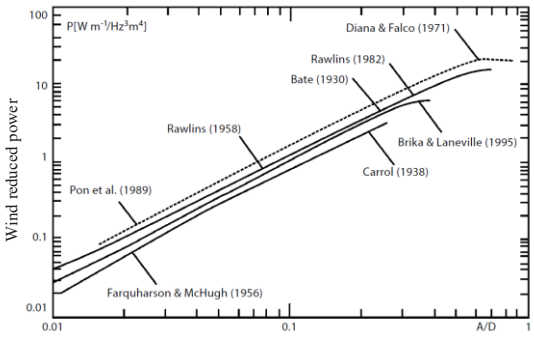

Non-dimensional amplitude A/D

Figure 1. Wind reduced power functions imparted to a vibrating cylinder versus non-dimensional amplitude A/D [4]

$$P_W = Lf^3D^4F\left(\frac{A}{D}\right) \tag{3}$$

Where L is the span length, D is conductor diameter, f is vibrating frequency, A is vibration amplitude (peak to peak), and $F(A/D)$ is a function of the non-dimensional vibration amplitude A/D. For the conventional and HTLS conductors of the same diameters, the wind power inputs can be considered the same. The study in [4] has summarised the empirical functions of wind power imparted to a vibrating cylinder against A/D, as shown in Fig. 1.

B. Conductor Self-damping Power

The conductor can self-damp part of the induced wind power through its vibration, reducing the vibration amplitude and thus the severity of the induced vibration fatigue. The mechanism of self-damping is a result of the inter-strand friction when the stranded conductor is bent. The self-damping power P_C can be expressed by (4).

$$P_C = k\frac{A^l f^m}{T^n}L \tag{4}$$

Where k is the factor of proportionality, L is the span length, f is vibrating frequency, T is the conductor tension, and A is vibration amplitude, l, m, and n are the exponents for amplitude, frequency, and tension, respectively. The differences in structure and materials of conventional and HTLS conductors result in different self-damping properties (l, m, and n). Thus the empirical values of l, m, and n are revealed by experiments, as reported in [4], [21].

C. Vibration Damper Dissipated Power

The modelling of the damper dissipated power P_D is very complicated because P_D is nonlinear against the vibration amplitude of conductor vibration. Many numerical models have been proposed, as in [13]–[16] and [22], while they are dedicated to Stockbridge dampers and cannot be used for other dampers. Therefore, an empirical method in [10] is used to calculate P_D for any vibration amplitude A, as in (5).

$$P_D = P_{D0}\left(\frac{A}{A_0}\right)^2 \quad (5)$$

Where P_{D0} is the base damper dissipated power, and A_0 is the base vibration amplitude (i.e., the amplitude used for the damper experimentation to produce the power dissipation characteristics of the damper).

D. *Conductor Vibration Induced Bending Stress & Life Expectancy Calculations*

With the maximum vibration amplitude (A) obtained from solving the EBP, the bending stress σ_a can be calculated by (6).

$$\sigma_a = \frac{1}{2} A\pi d E_a \sqrt{\frac{m}{\mathrm{EI}_{\min}}} f \quad (6)$$

Where E_a is Young's modulus of outer-layer wire material, d is the diameter of the outer layer wire, f is vibrating frequency, A is vibration amplitude, m is the conductor mass per unit length, $\mathrm{EI}_{\min}$ is the conductor minimum bending stiffness. For the conventional and HTLS conductors, Young's modulus is the same, since both conductors use aluminium as outer stranding material. However, their outer-layer wire diameter and bending stiffness are different (due to the structure, core material, and cross-sectional area differences).

Once the bending stress is known using (6), the estimated number of conductor vibration cycles to failure at each vibration frequency can be calculated using S-N graphs (i.e., Stress against number of vibration cycles to failure). Finally, the variation of wind speed is considered when calculating the aeolian vibration life expectancy of conductors. Weibull distribution is used to define the probability distribution of wind speed with its cumulative distribution function shown in (7).

$$P(U \le U_0) = 1 - \exp[-(U_0 / c_W)^{k_W}] \quad (7)$$

Where $P(U \leqslant U_0)$ is the probability that wind velocity U is less than U_0, k_W and c_W are the shape and scale parameters of Weibull distribution, respectively. Combining the number of vibration cycles to failure at each vibration frequency and the wind speed distribution in a certain area, the life expectancy of the conductor deployed at this area can be estimated.

III. Conventional vs. HTLS Case Study Results

The EBP method is well established for conventional conductors but it has not been used for HTLS conductors modelling. Therefore, EBP could be used to facilitate the understanding on the vibration and fatigue performance difference between conventional and HTLS conductors. The aeolian vibration amplitudes and the associated fatigue risks are calculated for a conventional ACSR conductor and a HTLS ACCC conductor. The specifications of the two types of conductors are given in Table I, with the diameters of these conductors being the same for comparison reason.

TABLE I. Parameters for Modelling of ACSR and ACCC

Parameters	ACSR	ACCC
Number of wires (Core/Aluminium)	7 / 45	1 / 37
Overall Diameter (mm)	29.9	29.9
Sectional area (mm^2)	528.2	655.38
Mass per unit length (kg/km)	1646	1753
Rated breaking strength (kN)	121.8	186.66

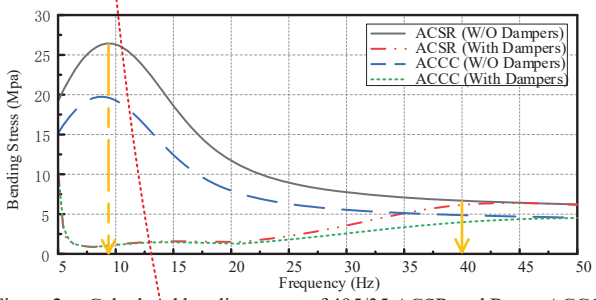

Figure 2. Calculated bending stress of 495/35 ACSR and Rome ACCC at 20%RBS

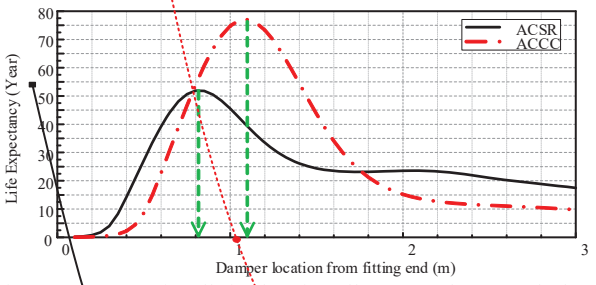

Figure 3. Damper installation location effect on conductor's calculated life expectancy

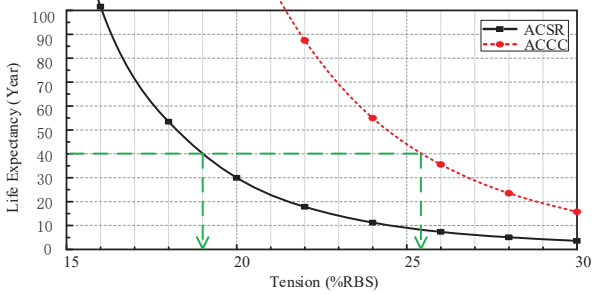

Figure 4. Calculated conductor life expectancy at various tension levels

The experimental data of the Stockbridge damper in [23] is used as base to calculate P_D and located at 1 m away from span-end for both conductors. According to laboratory tests, the ACCC power dissipated by self-damping is 5-10 times higher than ACSR conductor at the same conductor diameters and test condition [24]. The S-N curve is defined by CIGRE criterion in [25] known as CIGRÉ Safe Border Line (CSBL) and serves as a conservative prediction. The annual wind velocity profiles over land are obtained from [26].

In Fig. 2, it is obvious that the wind-induced aeolian vibrations are critical at low frequency (5-20 Hz, peak around 10 Hz), and deploying dampers can dramatically reduce the bending stress, for both ACSR and ACCC. However, the effect of the damper gradually drops with the increase in

vibration frequency, as the vibration amplitude decrease (with the increase of wind excitation frequency) leading to a reduction of damper power dissipation. Compared to ACSR, the bending stresses of the ACCC in full range without dampers and at frequency over 40 Hz with dampers are around 25% less due to its better self-damping performance.

The optimal location of the dampers for both conductor types are investigated. As shown in Fig. 3, the optimal damper location for the conventional ACSR is 0.8 m from the span-end, while the value for HTLS ACCC is 1.1 m. It shows that the optimal damper location for the novel HTLS ACCC is not the same as the conventional ACSR. Neglecting this difference can result in the reduction of HTLS ACCC life expectancy by around 30%.

The life expectancy of the two conductors at tension levels ranging from 15-30% Rated-Breakage-Strength (RBS) are shown in Fig. 4. It should be noticed that life expectancy above 100 years is neglected. As mentioned in Fig. 2, the bending stress of ACCC is lower than ACSR at the same tension level, and thus the ACCC has higher life expectancy than ACSR as shown in Fig. 4. It is also found in Fig. 4 that as the tension increases, the ACCC reducing life expectancy is delayed by 6%RBS (later drop) compared to the ACSR reducing life expectancy. Assuming that the expected life of a typical OHL conductor is 40 years, the installation tension for the ACSR is 19% RBS, while the value for ACCC is 6% more (25% RBS). Thus, the sag of ACCC is much lower compared to ACSR, at the same expected life and current flow, resulting in greater clearance and the potential of increasing ampacity without violating the clearance.

IV. Conductor Life Expectancy: Semi-Analytical Data-Driven Modelling Method

HTLS conductors have different structure, materials, and damping property and for this reason, the conversional modelling method may not predict accurately the life expectancy of HTLS conductors. Therefore, a semi-analytical modelling method is proposed aiming at improving the EBP to predict HTLS conductor's performance and ultimately minimize the prediction error. The proposed method is based on EBP assumptions with the major difference from other existing models being the integration of a calibration step based on experimental data, which can increase method's accuracy. The prediction error mainly is due to the conductor bending stiffness used in conventional EBP method, which is based on the minimum bending stiffness assumption and overestimating conductor's bending stress. The effect of bending stiffness on calculated results is also discussed in subsection IV.B.

A. Modelling Framework

The framework of the proposed model is shown in Fig. 5, including an initialization layer, three calculation layers, and an output layer. The input and output layers are the input OHL conductor system and damping specifications and output the predicted life expectancy, respectively. The three calculation layers are meant to calculate the bending stress of conductor without damper (layer 1), bending stress of conductor with damper (layer 2), and conductor life expectancy (layer 3). The input data include environmental data (e.g., location, temperature), conductor data (e.g. geometry, materials, bending stiffness), and installation data (e.g. tension level, location of dampers). The calculation layer 1 and 2 are the layers for calculating and calibrating the conductor self-damping and damper dissipation power respectively.

The bending stresses are calculated by vibration amplitude which is from EBP method based on the self-damping and damper data from experimental tests. Then the calculated stress is compared to the direct stress measurements form the test with the use of strain gauges. If the two results are different, the calibration (correction) is introduced to make the calculation and measurement results equal by calibrating the key parameters or importing the experimental correction coefficient. In calculation layer 3, the conductor life expectancy is determined through calculations of the fatigue modelling data (e.g., S-N graph, material properties). The fatigue calculation method is calibrated by comparing the result of the fatigue test to calculation result.

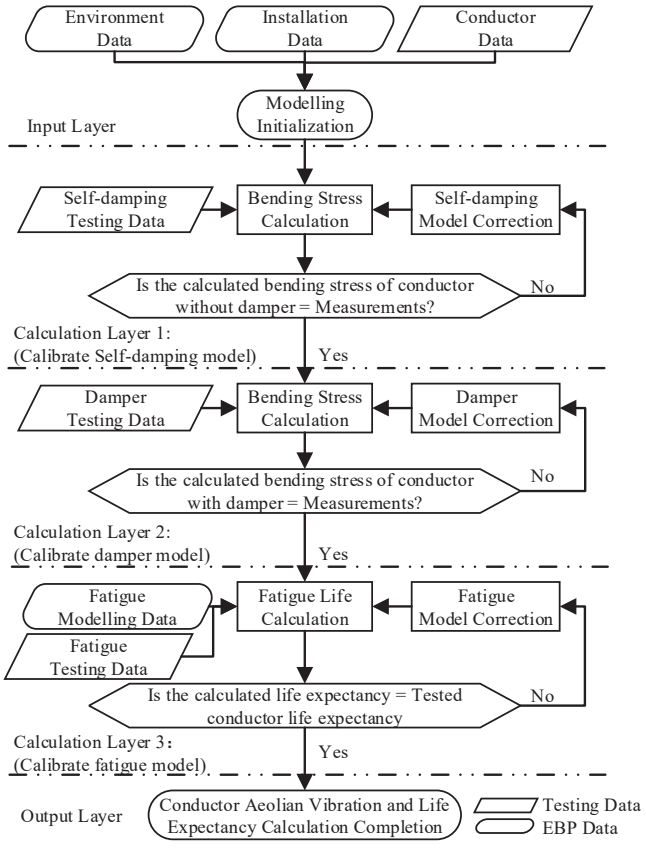

Figure 5. Conductor life expectancy modelling framework

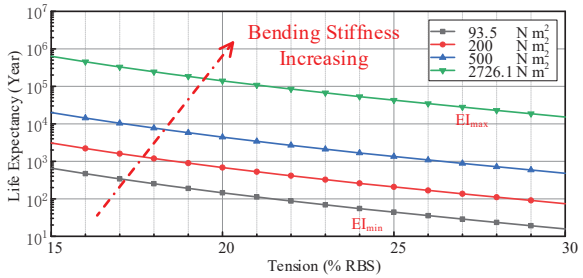

Figure 6. Effect of bending stiffness on ACCC life expectancy

B. *Effect of Bending Stiffness on Modelling Results*

Bending stiffness is an important parameter for calculating the bending stress and then life expectancy from the vibration amplitude to distinguish the performance of the different conductor geometries and sizes. Normally, the minimum bending stiffness assumption (EI_{min}) is used as a common practice. However, this is not accurate for all conductors because the minimum bending stiffness value assumes the sum of flexural rigidities of individual wires in the conductor with the assumption "wires loose"; no inter-strand friction. The results of life expectancy varying tension at different bending stiffness levels within the maximum and minimum range are shown in Fig. 6.

The maximum and minimum EI is 2726.1 and 93.5 $N{\cdot}m^2$, respectively. With the increase in flexure rigidity, life expectancy keeps decreasing dramatically. The life expectancy at 25%RBS is 44 years with the EI_{min} assumption (93.5 $N{\cdot}m^2$ in Fig. 6). When the EI is increased to 200 $N{\cdot}m^2$, the life expectancy is around 200 years. With the EI_{min} assumption, the calculated life expectancy is underestimated. Finally, the tension of HTLS conductors will be set lower and cannot be utilized effectively. To resolve this problem, the experimental method in [27] can measure the real EI of the conductor and optimize the modelling of various conductor geometries under different operating conditions.

V. Conclusions and the Future Works

In this paper, the aeolian vibration and life expectancy of ACCC and ACSR are calculated based on EBP method, with key assumptions stated. The results showed that for the same conductor size at the same installation conditions (tension in %RBS), the bending stress of Rome ACCC is 25% less than the 495/35 ACSR. Thus, ACCC has longer life (than ACSR) at the same installation conditions. It is also found that the optimal damper installation location is different for ACCC. Using the ACSR recommendations for the damper installation onto the ACCC can reduce ACCC's life expectancy by 30%. ACCC self-damping performance can allow for increasing installation tensions (i.e., 6% RBS more than ACSR) with the same useful life as its equivalent ACSR; thus allowing higher power transfer capacities for the same OHL system.

A data-driven, semi-analytical modelling framework is suggested as a potential solution to improve accuracy of EBP for predicting HTLS conductors' aeolian vibration amplitude and life expectancy. Future work includes additional experimental tests (on self-damping, damper location, and fatigue) to advance this proposed framework and its application to different HTLS conductors.

References

[1] R. V. Jones and K. J. Lomas, "Determinants of high electrical energy demand in UK homes: Socio-economic and dwelling characteristics," *Energy Build.*, vol. 101, pp. 24–34, May 2015.

[2] B. J. Pierre and G. T. Heydt, "Increased ratings of overhead transmission circuits using HTLS and compact designs," 2012.

[3] I. Hathout, K. Callery, J. Trac, and T. Hathout, "Impact of Thermal Stresses on the End of Life of Overhead Transmission Conductors," in *IEEE Power and Energy Society General Meeting*, Dec. 2018, vol. 2018-August.

[4] CIGRE, "Overhead Lines International Council on Large Electric Systems (CIGRE) Study Committee B2: Overhead Lines."

[5] P. Line Aeolian Vibrations and P. J-L Lilien, "Vibrations_eoliennes_intro," 2013.

[6] L. Li, Z. Zhang, and N. Xu, "Research on Aeolian Vibration Fatigue Life of Conductors," Apr. 2017, pp. 181–189.

[7] H. WOlF, B. AduM, damir SeMenSKi, dragan PuSTAić, F. strojarstva brodogradnje, and S. Zagrebu, "Using the Energy Balance Method in Estimation of Overhead Transmission Line Aeolian Vibrations," Hrvatski strojarski i brodograđevni inženjerski savez, Oct. 2008.

[8] G. Diana, A. Manenti, and C. RAWLINS, *Modelling of aeolian vibrations of single conductors: assessment of the technology*. 1998.

[9] G. Diana, "Modelling of Vibrations of Overhead Line Conductors Assessment of the Technology International Council on Large Electric Systems (CIGRE) Working Group B2.46."

[10] M. L. Lu and J. K. Chan, "An efficient algorithm for Aeolian vibration of single conductor with multiple dampers," *IEEE Trans. Power Deliv.*, vol. 22, no. 3, pp. 1822–1829, Jul. 2007.

[11] A. Rezaei and M. H. Sadeghi, "Aeolian Vibrations of Transmission Line Conductors with More than One Damper," *Int. J. Eng.*, vol. 28, no. 10, pp. 1515–1524, Oct. 2015.

[12] G. Diana, A. Cigada, M. Belloli, and M. Vanali, "Stockbridge-type damper effectiveness evaluation: Part I - Comparison between tests on span and on the shaker," *IEEE Trans. Power Deliv.*, vol. 18, no. 4, pp. 1462–1469, Oct. 2003.

[13] G. Diana, A. Manenti, C. Pirotta, and A. Zuin, "Stockbridge-type damper effectiveness evaluation: Part II - The influence of the impedance matrix terms on the energy dissipated," *IEEE Trans. Power Deliv.*, vol. 18, no. 4, pp. 1470–1477, Oct. 2003.

[14] S. Langlois and F. Legeron, "Prediction of aeolian vibration on transmission-line conductors using a nonlinear time history model - Part II: Conductor and damper model," *IEEE Trans. Power Deliv.*, vol. 29, no. 3, pp. 1176–1183, Jun. 2014.

[15] S. Langlois and F. Legeron, "Prediction of aeolian vibration on transmission-line conductors using a nonlinear time history model - Part I: Damper model," *IEEE Trans. Power Deliv.*, vol. 29, no. 3, pp. 1168–1175, 2014.

[16] O. Barry, R. Long, and D. Oguamanam, "Simplified Vibration Model and analysis of a single-conductor transmission line with dampers," *Proc. Inst. Mech. Eng. Part C J. Mech. Eng. Sci.*, vol. 231, no. 22, pp. 4150–4162, Nov. 2017.

[17] S. Guérard, B. Godard, and J. L. Lilien, "Aeolian vibrations on power-line conductors, evaluation of actual self damping," *IEEE Trans. Power Deliv.*, vol. 26, no. 4, pp. 2118–2122, Oct. 2011.

[18] W. Xie, Z. Zhang, N. Xu, L. Li, Z. Wang, and X. Luo, "Research on Aeolian Vibration of a Conductor Based on Finite Particle Method."

[19] S. Goudreau, F. Lévesque, and A. Cardou, "Analysis of variable amplitude loading fatigue tests on overhead conductor using palmgren-Miner rule."

[20] K.-H. Chang, "Fatigue and Fracture Analysis," in *e-Design*, Elsevier, 2015, pp. 463–521.

[21] *664-1993 IEEE Guide for Laboratory Measurement of the Power Dissipation Characteristics of Aeolian Vibaration*. .

[22] C. B. Rawlins, "The long span problem in the analysis of conductor vibration damping," *IEEE Trans. Power Deliv.*, vol. 15, no. 2, pp. 770–776, Apr. 2000.

[23] IEC, *IEC 62567：Methods for testing self-damping characteristics of conducto*. 2013.

[24] *Engineering Transmission Lines with High Capacity Low Sag ACCC Conductors*. 2011.

[25] CIGRE, "Recommendations for the evaluation of the lifetime of transmission line conductors," *Electra*, 1979.

[26] C. L. Archer and M. Z. Jacobson, "Evaluation of global wind power," *J. Geophys. Res*, vol. 110, p. 12110, 2005.

[27] F. Lévesque, S. Goudreau, S. Langlois, and F. Légeron, "Experimental Study of Dynamic Bending Stiffness of ACSR Overhead Conductors."